

A Quad-band Rectifier Design with Improved Matching Bandwidth for RF Energy Harvesting Applications

Talal Skaik

Electrical Engineering Department
Islamic University of Gaza, P.O. Box 108
Gaza, Palestine
talalskaik@gmail.com

Abstract—A quad-band energy harvester is proposed here. The harvester is formed of rectifiers and matching circuits at different frequency bands: GSM-900 (890-960 MHz), GSM-1800 (1800-1870 MHz), ISM 2.45 GHz (2.45-2.457 GHz) and LTE-band 7 (2.6-2.67 GHz). The harvester is formed of two dual-band matching circuits and two rectifiers instead of the conventional design with four single-band matching circuits and four rectifiers. The matching circuits are designed with improved matching bandwidth by employing several microstrip stubs to compensate for the limited matching bandwidth of the non-linear rectifier. Each rectifier is a four-stage voltage doubler with HSMS 285x Schottky diodes. The RF-DC conversion efficiency is simulated over frequency for various input power levels.

Keywords—Energy harvesting, Matching circuit, Multi-band, Quad-band, Rectifier.

I. INTRODUCTION

Recently, there is an increasing interest in harvesting of ambient energy available in different frequency bands. Energy harvesters can be used as power sources for small devices and they consist mainly of an antenna that captures RF energy and the antenna is connected to a rectifier via matching circuit. The rectifier circuit is used to convert the received AC signal into a DC signal and it usually consists of Schottky diodes that have impedances dependent on frequency as well as the input RF power. The matching circuit is used to match the input impedance of the rectifier to that of the antenna to achieve maximum power transfer.

There has been extensive research on energy harvesting systems operating on single band [1]-[6]. In [3], an antenna array with 10.67 dBi gain is proposed for harvesting at 915 MHz. In [4], a rectifier antenna is proposed for energy harvesting at 2.45 GHz to capture WiFi signals. Since the ambient energy available in single band is very small and not sufficient for real applications, more research is carried out on dual-band and multi-band harvesting circuits. Generally, in multi-band systems more energy can be captured from various low-density power sources.

Several dual-band harvesting circuits have been proposed in literature for different frequency bands: GSM-1800 and

UMTS-2100 in [7], GSM-900 and GSM-1800 in [8], [9] and 915 MHz and 2.45 GHz in [10]. Those harvesters are designed with dual-band matching circuits formed from short/open stubs and/or lumped elements.

Some more research has been done on multiband harvesters to capture more energy. In multiband harvesting, the circuit generally becomes more complicated and challenging in design. Two general approaches to design multi-band harvesting circuits can be followed. The first is to design separate rectifiers with single matching network for each rectifier then combine the DC outputs of the rectifiers together. The second design approach is based on single rectifying circuit connected to a multiband matching circuit that can be complicated and challenging in design.

Broadband antennas [11], [12] and multiband rectifier circuits [13]-[16] have been proposed in literature for RF energy scavenging. A tri-band rectifier is proposed for energy harvesting at 1050 MHz, 2050 MHz and 2600 MHz [13]. In [14] a four-band harvester is designed at GSM 900, GSM 1800, UMTS and WiFi bands. In [15], a tetra-band rectifier antenna is proposed to harvest RF energy and it works at GSM 900, GSM 1800, UMTS and WiFi. Moreover, a six band harvester is proposed for RF energy harvesting in [16].

It is generally noticed from literature review on single band and multiband harvesters that proposed matching circuits are designed over narrow bands and do not cover the whole standard allocated frequency bands. As a result, less energy is captured with those narrow band matching networks.

In the current work, a quad-band harvester is proposed with some features and the proposed circuit configuration is depicted in Fig. 1. Two dual-band matching circuits with two rectifiers are used instead of the regular circuit design with four single-band matching circuits and four rectifiers. The main focus in this paper is the proposed matching circuits that provide improved matching bandwidth over the whole allocated standard bands. A wideband antenna can be used to pick electromagnetic waves of many systems: GSM-900 (890-960 MHz), GSM-1800 (1800-1870 MHz), ISM 2.45 GHz (2.45-2.457 GHz) and LTE- band 7 (2.6-2.67 GHz).

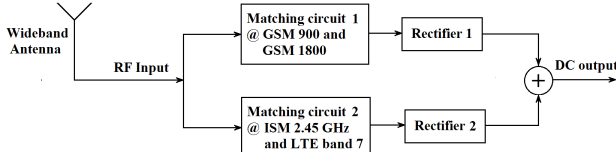


Fig. 1. Block diagram of the proposed quad-band harvesting system.

Since it is complex to design a single matching circuit at four-bands, two dual-band matching circuits are designed in the current work. The first matching circuit is designed at GSM-900 and GSM-1800, while the second circuit is designed at ISM 2.45 GHz and LTE band 7. Two identical four-stage rectifier circuits are used to convert the received AC signal into DC signal and the outputs of both rectifiers are combined to yield a DC output.

II. CIRCUIT DESIGN

The whole harvesting network is sub-divided into two separate networks in Fig. 2 and Fig. 3 each operating at two frequency bands. Each network is designed individually and then the two networks are combined together to form the whole harvester circuit in Fig. 4. Fig. 2 exhibits circuit diagram of a four-stage rectifier and a matching circuit at GSM-900 and GSM-1800. The diode used here in the rectifier circuit is HSMS 2852 Schottky that has high switching speed and low cutoff voltage which makes it good choice for rectification of high frequency and low power signals. The circuit is simulated using ADS 2015 from Agilent Technologies Inc where the diode is inserted into design from library as a package of series pair. The diode parameters are: $R_s = 25 \Omega$, $C_{j0} = 0.18 \text{ pF}$, $B_V = 3.8 \text{ V}$, $I_S = 3 \times 10^{-6} \text{ A}$, $I_{BV} = 3 \times 10^{-4} \text{ A}$ and $N = 1.06$.

A. Rectifier Circuit Input Impedance

The rectifier circuit is firstly simulated without matching circuits to obtain input impedance at different frequencies: 950 MHz, 1830 MHz, 2.45 GHz and 2.62 GHz. Smith Chart of the simulation results along with input impedance at those frequencies is presented in Fig. 5 and the return loss is shown in Fig. 6. The port impedance is set to 100Ω in simulation and subsequently each matching circuit will be designed to transform the complex input impedance of each rectifier to 100Ω . Eventually after combining the two circuits in Fig. 2 and Fig. 3 via a T-junction, the input impedance of the whole harvester circuit will be 50Ω as resultant of two 100Ω shunt input impedances of the two matching circuits.

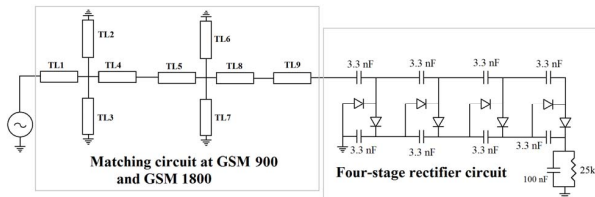


Fig. 2. Circuit diagram of the rectifier and matching circuit at GSM-900 and GSM-1800.

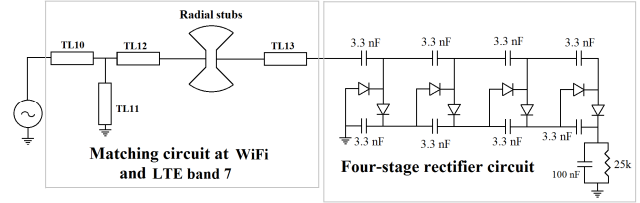


Fig. 3. Circuit diagram of the rectifier and matching circuit at WiFi and LTE band 7.

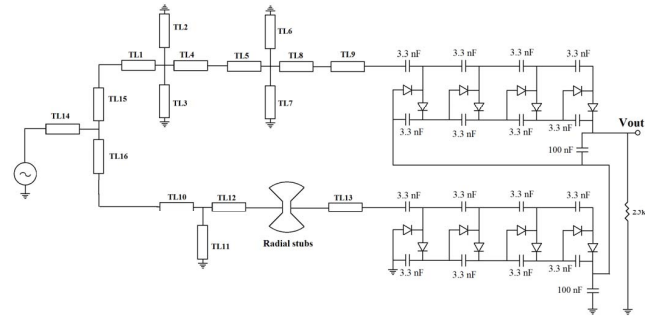


Fig. 4. Circuit diagram of the whole matching and rectifier system.

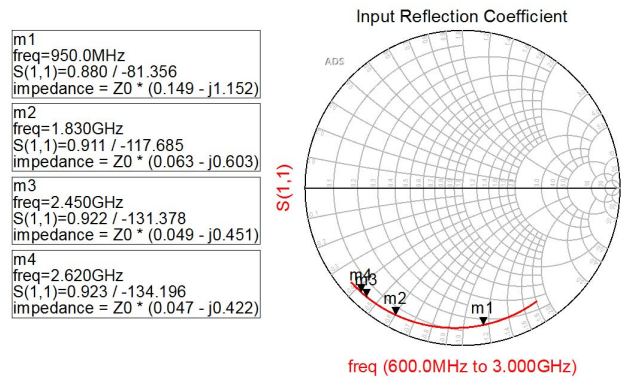


Fig. 5. Smith chart simulation results of rectifier circuit

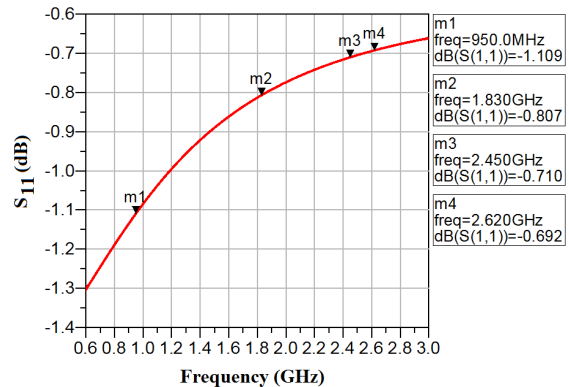


Fig. 6. Simulated S_{11} response of rectifier (without matching circuit).

B. Simulation of GSM-900 and GSM-1800 Circuit

The circuit in Fig. 2 is formed of a four-stage rectifier and a dual-band matching circuit at GSM-900 and GSM-1800. The matching circuit is formed of transmission lines (TL1, TL4,

TL5, TL8 and TL9) and four short-circuited stubs (TL2, TL3, TL6, and TL7) and its purpose is to transform the complex impedance of the rectifier to a 100Ω . The additional stubs and transmission lines here in the proposed design increase the matching bandwidth and achieve dual-band operation and thus increasing the captured power. The use of single stubs in matching circuits usually yields narrow matching bandwidth and hence additional stubs are used here. Two parallel stubs (TL2 and TL3) are tuned at the GSM-900 band and the other two stubs (TL6 and TL7) are tuned at the GSM-1800 band and thus widening the matching bandwidth at each band.

The simulated reflection coefficient (S_{11}) at the input of the matching circuit after optimizing the lengths and widths of the transmission lines is shown in Fig. 7. It can be noticed from the results that matching is achieved at the desired frequency bands GSM-900 and GSM-1800. The 6-dB matching bandwidth extends from 895 MHz to 965 MHz in GSM-900 band and from 1805 MHz to 1875 MHz in GSM-1800 band. Smith chart simulation result is depicted in Fig. 8.

C. Simulation of ISM 2.45 GHz and LTE Band 7 Circuit

The other circuit formed of a four-stage rectifier and dual-band matching network at WiFi and LTE band 7 is shown in Fig. 3. The matching circuit to a 100Ω consists of transmission lines (TL10, TL12 and TL13), a short-circuited stub TL11 and two radial stubs. The circuit is optimized using ADS software and the simulated S_{11} response is depicted in Fig. 9. It can be noticed that the 6-dB matching bandwidth extends from 2.41 GHz to 2.68 GHz and thus covering WiFi and LTE band 7 frequency bands. Smith chart simulated results are depicted in Fig. 10.

D. Simulation of Quad-band Rectifier Harvesting Circuit

The final quad-band harvester configuration is now formed by combining the circuits in Fig. 2 and Fig. 3 using a T-junction as exhibited in Fig. 4. The T-junction is represented here by the transmission lines: TL14 with characteristic impedance of $Z_0=50 \Omega$ and the lines TL15 and TL16 each with characteristic impedance of $Z_0=100 \Omega$.

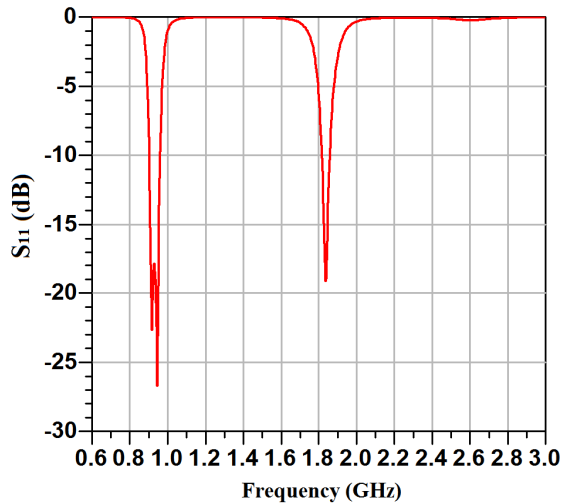


Fig. 7: Simulation result of S_{11} for circuit in Fig. 2.

The simulated reflection coefficient S_{11} for the final proposed configuration is presented in Fig. 11 and it can be noticed that matching over the four bands is achieved. The matching circuit is designed with microstrip lines on a substrate FR-4 with dielectric constant $\epsilon_r=4.1$ and thickness $h=1.6$ mm. The final dimensions of the lengths and widths of the microstrip transmission lines in the overall circuit in Fig. 4 are listed in Table I and the radial double shunt stub has radius of 14.939 mm and angle of 89° .

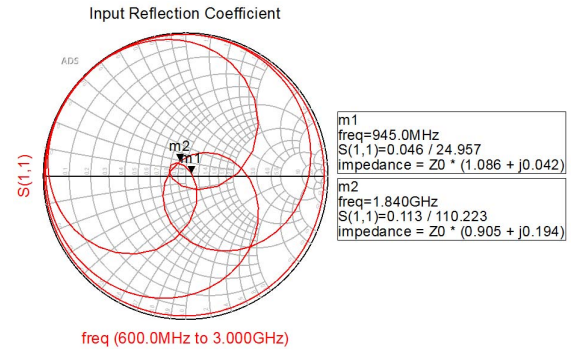


Fig. 8: Smith chart simulation result for circuit in Fig. 2.

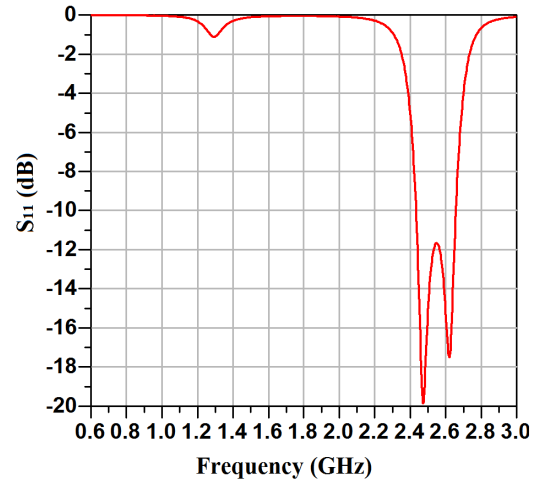


Fig. 9: Simulation result of S_{11} for circuit in Fig. 3.

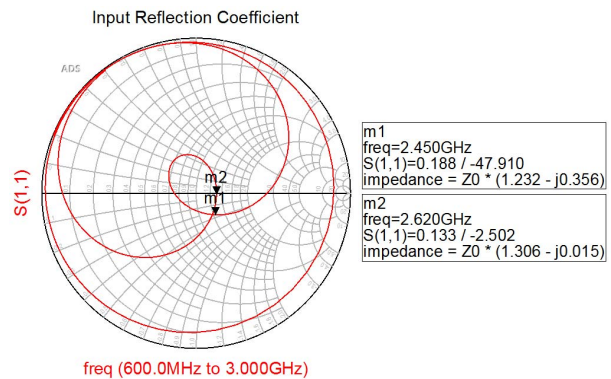


Fig. 10: Smith chart simulation result for circuit in Fig. 3.

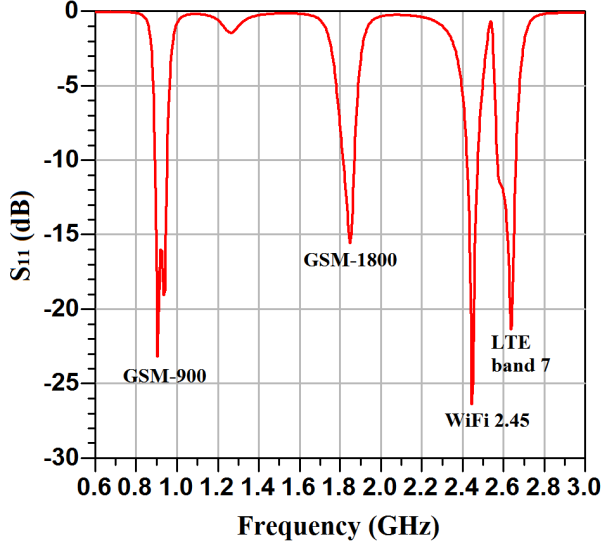


Fig. 11: Simulation result of S_{11} for circuit in Fig. 4.

TABLE I
DIMENSIONS OF MICROSTRIP LINES IN CIRCUIT

Tr. Line	Length (mm)	Width (mm)	Tr. Line	Length (mm)	Width (mm)
TL1	3.027	0.765	TL9	9.738	0.827
TL2	19.3696	0.751	TL10	3.600	0.765
TL3	26.000	2.002	TL11	28.053	1.672
TL4	49.588	2.710	TL12	39.704	7.000
TL5	25.374	2.048	TL13	5.402	2.392
TL6	06.760	5.891	TL14	30.00	3.226
TL7	04.000	0.894	TL15	8.283	0.765
TL8	25.494	12.214	TL16	24.753	0.765

The circuit has been simulated using Harmonic Balance (HB) simulation in ADS to obtain the output voltage for different input power levels from -20 dBm to +10 dBm. The simulation results are shown in Fig. 12 for the desired frequencies: 950 MHz, 1835 MHz, 2450 MHz and 2620 MHz and the output voltage is taken at a 25 k Ω load. The output DC voltage clearly increases as the input power increases. Furthermore, the RF-DC conversion efficiency has been calculated from HB simulation results by,

$$\eta(\%) = \frac{V_L^2}{R_L} \times \frac{1}{P_{in}} \times 100 \quad (1)$$

where V_L is the output DC voltage on load resistance R_L . The efficiency results versus frequency are presented in Fig. 13 for load resistance $R_L=25$ k Ω and for input power levels of -10 dBm, 0 dBm and +10 dBm. The results show that the efficiency varies with frequency and the highest efficiency is obtained at frequencies where matching is achieved.

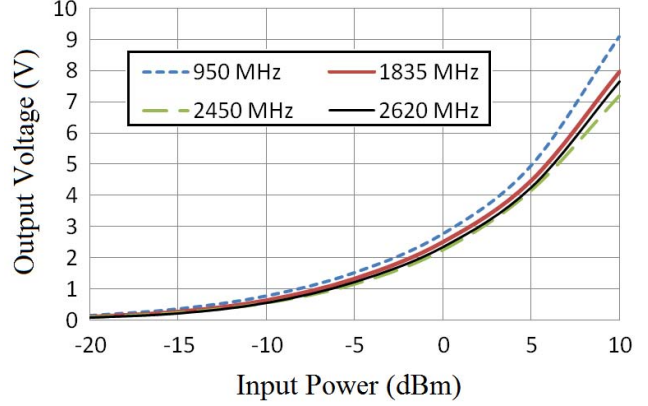


Fig. 12: Output DC voltage on 25 k Ω versus input power levels

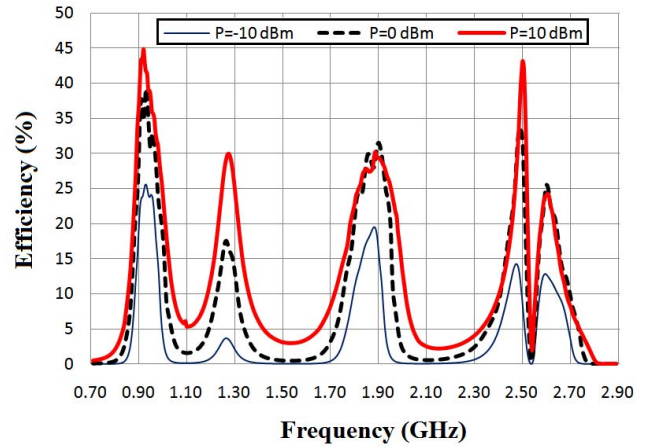


Fig. 13: Efficiency versus frequency for different input power levels with output voltage on 25 k Ω .

Moreover, it can be noticed in Fig. 13 that the lowest efficiency is obtained at input power of -10 dBm while it is higher for larger input power levels. The highest efficiency at GSM-900 band for input powers of -10 dBm, 0 dBm and +10 dBm is 25.5%, 39.3% and 44.8% respectively, and at GSM-1800 band it is 18.8%, 30% and 27.5% respectively. Moreover, the highest efficiency at the ISM 2.45 GHz band is 14.1%, 26.3% and 28% for input power of -10 dBm, 0 dBm and +10 dBm respectively and at the LTE band 7 it is 12.7%, 25.5% and 24.2% respectively. The conversion efficiency of the proposed circuit is largely dependent on the load resistance. Different values of loads have been considered in HB simulations and a 25 k Ω load resistance is chosen as higher efficiency is obtained. It has to be mentioned that the simulation results above considered no losses in dielectric substrate (loss tangent = 0).

III. CONCLUSION

A quad band RF energy harvester is proposed here. It is designed of two dual-band rectifier circuits and two four-stage rectifiers. The proposed harvester operates at GSM-900 (890-960 MHz), GSM-1800 (1800-1870 MHz), ISM 2.45 GHz (2.45-2.457 GHz) and LTE- band 7 (2.6-2.67 GHz).

Impedance matching is achieved over the whole allocated standard frequency bands using microstrip shunt and radial stubs. The output DC voltage is simulated for single-tone input signals with input power levels from -20 dBm to +10 dBm and the results showed increase in output voltage when increasing the input power. The RF-DC conversion efficiency is simulated over frequency for different input power levels (-10 dBm, 0 dBm and +10 dBm). The simulations showed that higher efficiency is obtained with larger input power level.

REFERENCES

- [1] B. Merabet *et al.*, "Low-cost converter for harvesting of microwave electromagnetic energy," 2009 IEEE Energy Conversion Congress and Exposition, San Jose, CA, 2009, pp. 2592-2599.
- [2] S. Ladan, N. Ghassemi, A. Ghiotto and K. Wu, "Highly Efficient Compact Rectenna for Wireless Energy Harvesting Application," in IEEE Microwave Magazine, vol. 14, no. 1, pp. 117-122, Jan.-Feb. 2013.
- [3] F. Xie, G. M. Yang and W. Geyi, "Optimal Design of an Antenna Array for Energy Harvesting," in IEEE Antennas and Wireless Propagation Letters, vol. 12, pp. 155-158, 2013.
- [4] S. B. Alam, M. S. Ullah and S. Moury, "Design of a low power 2.45 GHz RF energy harvesting circuit for rectenna," 2013 International Conference on Informatics, Electronics and Vision (ICIEV), Dhaka, 2013, pp. 1-4.
- [5] Xuyue Wu, Junjun Wang, Mengxi Liu and Huan Liu, "A high efficiency rectifier for ambient RF energy harvesting at 940 MHz," 2016 IEEE International Conference on Microwave and Millimeter Wave Technology (ICMMT), Beijing, 2016, pp. 593-595.
- [6] M. Abdallah, J. Costantine, A. H. Ramadan, Y. Tawk and C. G. Christodoulou, "A new RF rectifier for energy harvesting with enhanced dynamic power range," 2016 IEEE International Symposium on Antennas and Propagation (APSURSI), Fajardo, 2016, pp. 605-606.
- [7] H. Sun, Y. x. Guo, M. He and Z. Zhong, "A Dual-Band Rectenna Using Broadband Yagi Antenna Array for Ambient RF Power Harvesting," in IEEE Antennas and Wireless Propagation Letters, vol. 12, pp. 918-921, 2013.
- [8] L. M. Borges *et al.*, "Design and evaluation of multi-band RF energy harvesting circuits and antennas for WSNs," 2014 21st International Conference on Telecommunications (ICT), Lisbon, 2014, pp. 308-312.
- [9] Z. Liu, Z. Zhong and Y. X. Guo, "Enhanced Dual-Band Ambient RF Energy Harvesting With Ultra-Wide Power Range," in IEEE Microwave and Wireless Components Letters, vol. 25, no. 9, pp. 630-632, Sept. 2015.
- [10] K. Niotaki, S. Kim, S. Jeong, A. Collado, A. Georgiadis and M. M. Tentzeris, "A Compact Dual-Band Rectenna Using Slot-Loaded Dual Band Folded Dipole Antenna," in IEEE Antennas and Wireless Propagation Letters, vol. 12, pp. 1634-1637, 2013.
- [11] M. Arrawatia, M. S. Baghini and G. Kumar, "Broadband Bent Triangular Omnidirectional Antenna for RF Energy Harvesting," in IEEE Antennas and Wireless Propagation Letters, vol. 15, pp. 36-39, 2016.
- [12] M. Arrawatia, M. S. Baghini and G. Kumar, "Broadband rectenna array for RF energy harvesting," 2016 IEEE International Symposium on Antennas and Propagation (APSURSI), Fajardo, 2016, pp. 1869-1870.
- [13] D. Wang and R. Negra, "Novel TriBand RF Rectifier Design for Wireless Energy Harvesting," GeMiC 2014; German Microwave Conference, Aachen, Germany, 2014, pp. 1-3.
- [14] V. Kuhn, C. Lahuec, F. Seguin and C. Person, "A Multi-Band Stacked RF Energy Harvester With RF-to-DC Efficiency Up to 84%," in IEEE Transactions on Microwave Theory and Techniques, vol. 63, no. 5, pp. 1768-1778, May 2015.
- [15] D. Masotti, A. Costanzo, M. D. Prete and V. Rizzoli, "Genetic-based design of a tetra-band high-efficiency radio-frequency energy harvesting system," in IET Microwaves, Antennas & Propagation, vol. 7, no. 15, pp. 1254-1263, 2013.
- [16] C. Song *et al.*, "A Novel Six-Band Dual CP Rectenna Using Improved Impedance Matching Technique for Ambient RF Energy Harvesting," in IEEE Transactions on Antennas and Propagation, vol. 64, no. 7, pp. 3160-3171, July 2016.